ELSEVIER

Journal of Structural Geology 30 (2008) 539–546

JOURNAL OF STRUCTURAL GEOLOGY

www.elsevier.com/locate/jsg

An analytical approach for determining strain ellipsoids from measurements on planar surfaces

Yehua Shan [a,b,*]

[a] Laboratory of Marginal Sea Geology, Guangzhou Institute of Geochemistry, Chinese Academy of Sciences, Wushan, Guangzhou City 510640, PR China

[b] Computational Geosciences Research Center, Central South University, Changsha City 410083, PR China

Received 18 March 2006; received in revised form 5 December 2006; accepted 14 December 2006
Available online 27 December 2006

Abstract

A new method is proposed to determine strain ellipsoids from measurements made on planar surfaces. It is similar in theory to that of Robin, P.-Y.F., [2002. Determination of fabric and strain ellipsoids from measured sectional ellipses – theory. Journal of Structural Geology 24, 531–544], but is more flexible and hence more applicable because it can incorporate different kinds of strain measurements, especially when only the pitches of the long/short axes of strain ellipses are measured on planar surfaces. It is not necessary to estimate both the relative and absolute strain ellipsoids at the same time, as Robin, P.-Y.F., [2002. Determination of fabric and strain ellipsoids from measured sectional ellipses – theory. Journal of Structural Geology 24, 531–544] and others did. The former may be estimated before the latter. The feasibility of the proposed method is demonstrated by three artificial examples and one real example.
© 2007 Elsevier Ltd. All rights reserved.

Keywords: Estimation; Strain ellipsoids; Sectional measurements; Strain markers

1. Introduction

One goal of structural geologists is to determine the finite strain that a rock underwent during plastic deformation, since this is important in reconstructing the deformation history the rock has been through. Strain markers such as deformed pebbles, particles, fossils, reduction spots, and so forth are useful strain recorders in nature. They are commonly used to estimate strain in rocks. Among the numerous measurement techniques available (e.g. Ramsay, 1967; Ramsay and Huber, 1983), most produce an estimate of a strain ellipse on a planar surface. Only a few lead to an estimate of the strain ellipsoid. However, these may not be applicable to sectional measurements of any kind, as will be described below. In this regard, it is common practice to construct the strain ellipsoid from measured ellipses on several planar surfaces. A key problem in constructing a strain ellipsoid is how to establish a strain tensor from the passive strain markers. This problem can be solved graphically through converting strain measurements on three non-parallel surfaces into their counterparts on three mutually perpendicular surfaces. In the latter case, the strain tensor is readily established from the converted values (Ramsay, 1967).

Alternatively, numerical algorithms (Shimamoto and Ikeda, 1976; Oertel, 1978; Milton, 1980; Gendzwill and Stauffer, 1981; Owens, 1984; Shao and Wang, 1984; De Paor, 1990; Robin, 2002) have been proposed for the same purpose. They differ in how they tackle the consistency of sectional data, as well as other aspects. Most use iteration to examine the best-fit strain ellipsoid. They are not completely robust in finding a local minimum to which the solution may proceed (Robin, 2002; see his brief review in the introduction). Robin (2002) proposed a direct and non-iterative algorithm that solves a set

* Corresponding author. Laboratory of Marginal Sea Geology, Guangzhou Institute of Geochemistry, Chinese Academy of Sciences, Wushan, Guangzhou City 510640, PR China. Tel.: +86 20 85290763; fax: +86 20 85290130.

E-mail address: shanyehua@yahoo.com.cn

0191-8141/$ - see front matter © 2007 Elsevier Ltd. All rights reserved.
doi:10.1016/j.jsg.2006.12.004

of linear equations obtained through minimizing the sum of norms of ‘‘error matrices’’ for a strain ellipsoid.

The main purpose of this study was to develop a new algorithm for determining analytically a strain ellipsoid from sectional data. The algorithm is somewhat similar, in terms of directness and a lack of need for iteration, to Robin's algorithm (2002), because both look for the solution through finding the global minimum. However, this one appears more flexible and, therefore, is more widely applicable, because sectional measurements of variable kinds may be incorporated together in the calculation of a strain ellipsoid.

The terms and symbols used in this paper are listed in Table 1.

2. Basic equations for sectional measurements

In the Cartesian system (Fig. 1), a strain ellipsoid is a quadric surface centered at the origin. It is described by the following equation:

$$\begin{bmatrix} x & y & z \end{bmatrix} \begin{bmatrix} b_{11} & b_{12} & b_{13} \\ b_{21} & b_{22} & b_{23} \\ b_{31} & b_{32} & b_{33} \end{bmatrix} \begin{bmatrix} x \\ y \\ z \end{bmatrix} = 1 \tag{1}$$

where x, y and z are the coordinates of a point on the ellipsoid. The middle matrix is symmetrical, so $b_{ij} = b_{ji}$ ($i, j = 1, 2, 3$). It is called the shape matrix (Shimamoto and Ikeda, 1976), or the inverse shape matrix (Wheeler, 1989). The principal axes of the ellipsoid have the same directions as the eigenvectors of the shape matrix, but different dimensions from the eigenvalues,

$$\varepsilon_1 = \frac{1}{\sqrt{b_3}},\ \varepsilon_2 = \frac{1}{\sqrt{b_2}},\ \varepsilon_3 = \frac{1}{\sqrt{b_1}} \tag{2}$$

where b_1, b_2, and b_3 are the corresponding eigenvalues of the shape matrix ($b_1 \geq b_2 \geq b_3 > 0$); ε_1, ε_2, and ε_3 are the corresponding magnitudes of the principal axes of the ellipsoid ($\varepsilon_1 \geq \varepsilon_2 \geq \varepsilon_3 > 0$).

We consider N strain measurements made directly, or otherwise calculated, on planar surfaces. On the i-th plane, we measure the dip direction (α_i) and dip angle (β_i) of the surface, and the pitch (θ_i) of the long axis of an ellipse on the surface, and/or the ratio (R_i) of the long axis to the short axis, and/or the magnitudes (l_{i1} and l_{i2}) of the short and long axes ($i = 1,2,\ldots,N$). The pitch is defined here as the intersection angle between the long axis of the ellipse and the western trend of the plane after it has been rotated about a vertical axis until it dips toward the north, or the X-axis (Fig. 1). For the sake of convenience, the axial lengths are referred to as those measured on planar surfaces through the center of the strain ellipsoid. It is necessary, as shown below, to have these data in order to estimate the absolute strain ellipsoid. However, measured strain ellipses on surfaces that do not cut through the center of the ellipsoid are very common in the field, and cannot be used directly for this purpose. They need to be modified to the strain ellipses on parallel planes through the center by multiplying them with a scale constant depending upon each measurement. Generally, it is difficult to gain the knowledge needed for modification in the field.

For each individual measurement, we can perform a series of rotations to transform a strain measurement plane into a horizontal one where the long axis of the strain ellipse is aligned

Table 1
List of symbols and their definitions

Symbols	Definitions	Comments
x, y, and z	Coordinates of a point on the ellipsoid in the real state.	Eqs. (1) and (4).
x', y', and z'	Coordinates of a point on the ellipsoid in the rotated state.	Eqs. (4) and (6).
b_{ij}	Elements of a shape matrix.	$i, j = 1,2,3$; Eqs. (1) and (7).
b'_{ij}	Elements of a transformed shape matrix.	See Section 2.
b	Normalized shape-matrix vector.	Eqs. (9), (11) and (12).
b^*	The relative solution of a shape-matrix vector.	Eq. (15).
$\overline{b}$	The absolute solution of a shape-matrix vector.	Eq. (15).
b_1, b_2, and b_3	Eigenvalues of a shape matrix.	$b_1 \geq b_2 \geq b_3 > 0$; Eq. (2).
ε_1, ε_2, and ε_3	Magnitudes of the principal axes of an ellipsoid.	$\varepsilon_1 \geq \varepsilon_2 \geq \varepsilon_3 > 0$; Eq. (2).
N	Number of strain measurements.	
α_i and β_i	Dip and dip angle of the i-th measured planar surface.	$i = 1,2,\ldots,N$; Eq. (3).
θ_i	Pitch of the long axis of a strain ellipse on the i-th planar surface.	$i = 1,2,\ldots,N$; Eq. (3).
R_i	Axial ratio of a strain ellipse on the i-th planar surface.	$i = 1,2,\ldots,N$; Eq. (3).
l_{i1} and l_{i2}	Half lengths of the long and the short axes of a strain ellipse on the i-th planar surface.	$i = 1,2,\ldots,N$; Eqs. (3), (6), (7a), (7b), and (16)–(17).
$T^{(i)}$	(1) Rotation matrix, and	Eq. (3).
$t_{ij}^{(k)}$	(2) Elements of a rotation matrix.	$i, j = 1,2,3$; $k = 1,2,\ldots,N$; Eqs. (3), (7)–(8), and (16)–(17).
v_i and w_i	Datum vectors.	$i = 1,2,\ldots,N$; Eqs. (3) and (10)–(13).
F	Objective function.	Eq. (12).
U	Datum matrix.	Eqs. (12) and (13).
A	A set of all strain measurements.	Eqs. (12)–(14).
A_i	Subset of measurements with different kinds of known variables.	$i = 1,2,3$; Eqs. (12)–(14).
k_i	Scale parameter.	Eqs. (15) and (17).
p_i and q_i		Eq. (17).

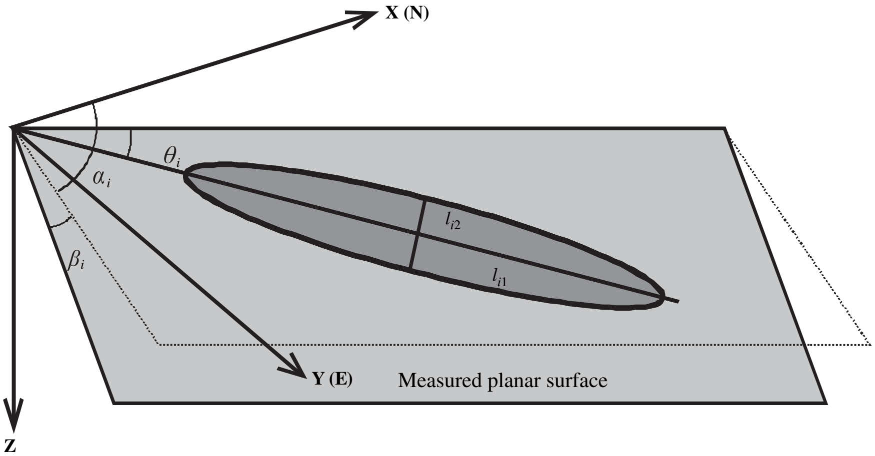

Fig. 1. Elements of strain measurements made on the planar surface in the Cartesian coordinate system. The rectangle, marked by three dashed lines and one thick line, represents a part of the horizon (namely, the $X-Y$ plane). See the text for symbol definitions.

with the X-axis (Fig. 1). This can be implemented by rotating around the Z-axis with an angle of $-\alpha_i$, around the Y-axis with an angle of $-\beta_i$, and finally around the Z-axis with an angle of $\theta_i - 90°$. Thus, we can use matrix $T^{(i)}$ to express these rotations.

$$T^{(i)} = \begin{bmatrix} t_{11}^{(i)} & t_{12}^{(i)} & t_{13}^{(i)} \\ t_{21}^{(i)} & t_{22}^{(i)} & t_{23}^{(i)} \\ t_{31}^{(i)} & t_{32}^{(i)} & t_{33}^{(i)} \end{bmatrix} = \begin{bmatrix} \cos\alpha_i & -\sin\alpha_i & 0 \\ \sin\alpha_i & \cos\alpha_i & 0 \\ 0 & 0 & 1 \end{bmatrix} \begin{bmatrix} \cos\beta_i & 0 & -\sin\beta_i \\ 0 & 1 & 0 \\ \sin\beta_i & 0 & \cos\beta_i \end{bmatrix} \begin{bmatrix} \cos(90° - \theta_i) & \sin(90° - \theta_i) & 0 \\ -\sin(90° - \theta_i) & \cos(90° - \theta_i) & 0 \\ 0 & 0 & 1 \end{bmatrix} \quad (3)$$

After applying the transformation operation defined in Eq. (3), a point (x, y, z) of the ellipsoid in the previous coordinate system is transformed into a new point (x', y', z') as follows:

$$[x \quad y \quad z]^{\mathrm{T}} = T^{(i)} [x' \quad y' \quad z']^{\mathrm{T}} \quad (4)$$

where superscript T is the operation of matrix transposition.

Inserting Eq. (4) into Eq. (1) and letting $z' = 0$ leads to the following equation:

$$[x' \quad y'] \begin{bmatrix} t_{11}^{(i)}t_{11}^{(i)}b_{11} + 2t_{11}^{(i)}t_{21}^{(i)}b_{12} + 2t_{11}^{(i)}t_{31}^{(i)}b_{13} & t_{11}^{(i)}t_{12}^{(i)}b_{11} + \left(t_{11}^{(i)}t_{22}^{(i)} + t_{21}^{(i)}t_{12}^{(i)}\right)b_{12} \\ + t_{21}^{(i)}t_{21}^{(i)}b_{22} + 2t_{21}^{(i)}t_{31}^{(i)}b_{23} + t_{31}^{(i)}t_{31}^{(i)}b_{33} & + \left(t_{11}^{(i)}t_{32}^{(i)} + t_{31}^{(i)}t_{12}^{(i)}\right)b_{13} + t_{21}^{(i)}t_{22}^{(i)}b_{22} \\ & + \left(t_{21}^{(i)}t_{32}^{(i)} + t_{31}^{(i)}t_{22}^{(i)}\right)b_{23} + t_{31}^{(i)}t_{32}^{(i)}b_{33} \\ \text{(symmetrical)} & t_{12}^{(i)}t_{12}^{(i)}b_{11} + 2t_{12}^{(i)}t_{22}^{(i)}b_{12} + 2t_{12}^{(i)}t_{32}^{(i)}b_{13} \\ & + t_{22}^{(i)}t_{22}^{(i)}b_{22} + 2t_{22}^{(i)}t_{32}^{(i)}b_{23} + t_{32}^{(i)}t_{32}^{(i)}b_{33} \end{bmatrix} \begin{bmatrix} x' \\ y' \end{bmatrix} = 1 \quad (5)$$

The strain ellipse on a plane in the new coordinate system is described by:

$$[x' \quad y'] \begin{bmatrix} l_{i2}^{-2} & 0 \\ 0 & l_{i1}^{-2} \end{bmatrix} \begin{bmatrix} x' \\ y' \end{bmatrix} = 1 \quad (6)$$

The above equation is valid only for strain measurements on the planes through the center of the strain ellipsoid, as was stated above. Strain measurements on the planes that do not pass the center are discussed in next section.

Because Eqs. (5) and (6) have the same shape matrix, we have the following expressions:

$$t_{11}^{(i)}t_{11}^{(i)}b_{11} + 2t_{11}^{(i)}t_{21}^{(i)}b_{12} + 2t_{11}^{(i)}t_{31}^{(i)}b_{13} + t_{21}^{(i)}t_{21}^{(i)}b_{22} + 2t_{21}^{(i)}t_{31}^{(i)}b_{23} + t_{31}^{(i)}t_{31}^{(i)}b_{33} = l_{i2}^{-2} \quad (7a)$$

$$t_{12}^{(i)}t_{12}^{(i)}b_{11} + 2t_{12}^{(i)}t_{22}^{(i)}b_{12} + 2t_{12}^{(i)}t_{32}^{(i)}b_{13} + t_{22}^{(i)}t_{22}^{(i)}b_{22} + 2t_{22}^{(i)}t_{32}^{(i)}b_{23} + t_{32}^{(i)}t_{32}^{(i)}b_{33} = l_{i1}^{-2} \quad (7b)$$

$$t_{11}^{(i)}t_{12}^{(i)}b_{11} + \left(t_{11}^{(i)}t_{22}^{(i)} + t_{21}^{(i)}t_{12}^{(i)}\right)b_{12} + \left(t_{11}^{(i)}t_{32}^{(i)} + t_{31}^{(i)}t_{12}^{(i)}\right)b_{13} + t_{21}^{(i)}t_{22}^{(i)}b_{22} + \left(t_{21}^{(i)}t_{32}^{(i)} + t_{31}^{(i)}t_{22}^{(i)}\right)b_{23} + t_{31}^{(i)}t_{32}^{(i)}b_{33} = 0 \quad (7c)$$

Until now this procedure closely parallels that of Robin (2002; Eq. 5) and Owens (1984; Eq. 19).

It is noteworthy that, where measured plane surfaces are principal planes, all non-diagonal elements in the shape matrix resulting from the transformation are zero. Let b'_{ij} stand for the elements of the transformed shape matrix. Because $b'_{13}=0$, and $b'_{23}=0$, we have two more independent linear equations. This is beyond the scope of this paper, and will not be discussed below.

Measurements on the plane surfaces that are not principal planes are the most common in the field. We now consider the minimal number of measurements of different types necessary to determine a strain ellipsoid. For one measurement with three known variables such as θ_i, l_{i1}, and l_{i2}, there are three independent linear Eqs. (7a)–(7c). Because the shape matrix (see Eq. (1)) has six unknown elements, two such independent measurements are required to determine an absolute strain ellipsoid.

Dividing Eq. (7a) by Eq. (7b) and inserting $R_i=l_{i1}/l_{i2}$ leads to the following equation:

$$\begin{aligned}&\left(t_{11}^{(i)}t_{11}^{(i)}R_i^2-t_{12}^{(i)}t_{12}^{(i)}\right)b_{11}+2\left(t_{11}^{(i)}t_{21}^{(i)}R_i^2-t_{12}^{(i)}t_{22}^{(i)}\right)b_{12}\\&+2\left(t_{11}^{(i)}t_{31}^{(i)}R_i^2-t_{12}^{(i)}t_{32}^{(i)}\right)b_{13}+\left(t_{21}^{(i)}t_{21}^{(i)}R_i^2-t_{22}^{(i)}t_{22}^{(i)}\right)b_{22}\\&+2\left(t_{21}^{(i)}t_{31}^{(i)}R_i^2-t_{22}^{(i)}t_{32}^{(i)}\right)b_{23}+\left(t_{31}^{(i)}t_{31}^{(i)}R_i^2-t_{32}^{(i)}t_{32}^{(i)}\right)b_{33}=0\end{aligned}\quad(7d)$$

Similarly, for a measurement with two known variables such as θ_i, and R_i, there are two independent linear Eqs. (7c) and (7d). But in this case, the number of unknown elements in the shape matrix is five. This indicates that at least three independent measurements are needed to determine a relative strain ellipsoid, including the directions and relative magnitudes of its maximum, intermediate and minimum axes.

For a measurement with only one known variable θ_i, there is just one linear Eq. (7c). At least five measurements of this kind are insufficient to determine a relative strain ellipsoid. They are intrinsically inadequate in the determination, even where more can be measured (see below), and must be used together with other kinds of measurements.

3. Analytical solution for a relative strain ellipsoid

For N strain measurements, as obtained above, we determine a set of linear equations for the shape matrix. There is an analytical solution for these equations if they are determined, or an optimal solution if they are over-determined. In the former case, the Gaussian elimination method may directly be used to solve the equations for the shape matrix. In the latter case, numerical algorithms are needed.

We assume that a set of strain measurements, either with two known variables such as θ_i and R_i or with one known variable θ_i, can lead to a set of over-determined linear Eqs. (7c) and (7d). These two kinds of equations have geometrical meaning in the six-dimensional space. The solution of the shape-matrix vector $b=[b_{11},b_{12},b_{13},b_{22},b_{23},b_{33}]^{\mathrm{T}}$ is perpendicular to the two respective kinds of datum vectors in the following.

$$\left[t_{11}^{(i)}t_{12}^{(i)},t_{11}^{(i)}t_{22}^{(i)}+t_{21}^{(i)}t_{12}^{(i)},t_{11}^{(i)}t_{32}^{(i)}+t_{31}^{(i)}t_{12}^{(i)},t_{21}^{(i)}t_{22}^{(i)},t_{21}^{(i)}t_{32}^{(i)}+t_{31}^{(i)}t_{22}^{(i)},t_{31}^{(i)}t_{32}^{(i)}\right]\quad(8a)$$

$$\begin{aligned}&\left[t_{11}^{(i)}t_{11}^{(i)}R_i^2-t_{12}^{(i)}t_{12}^{(i)},\ 2\left(t_{11}^{(i)}t_{21}^{(i)}R_i^2-t_{12}^{(i)}t_{22}^{(i)}\right),\ 2\left(t_{11}^{(i)}t_{31}^{(i)}R_i^2-t_{12}^{(i)}t_{32}^{(i)}\right),\right.\\&\left.t_{21}^{(i)}t_{21}^{(i)}R_i^2-t_{22}^{(i)}t_{22}^{(i)},\ 2\left(t_{21}^{(i)}t_{31}^{(i)}R_i^2-t_{22}^{(i)}t_{32}^{(i)}\right),\ t_{31}^{(i)}t_{31}^{(i)}R_i^2-t_{32}^{(i)}t_{32}^{(i)}\right]\end{aligned}\quad(8b)$$

In order to obtain a solution for the relative shape matrix, we may assume that the shape-matrix vector can be located on a unit hyper-sphere centered at the origin. This assumption leads to the following expression:

$$b^{\mathrm{T}}b=1\quad(9)$$

We can normalize the above two datum vectors by their lengths so that the modified datum vectors are:

$$v_i=[v_{i1},v_{i2},v_{i3},v_{i4},v_{i5},v_{i6}]\quad(10a)$$

$$w_i=[w_{i1},w_{i2},w_{i3},w_{i4},w_{i5},w_{i6}]\quad(10b)$$

This normalization will guarantee the same weight of each datum vector on the value of the objective function defined below.

Eqs. (7c) and (7d) can be rewritten as:

$$v_i^{\mathrm{T}}b=0\quad(11a)$$

$$w_i^{\mathrm{T}}b=0\quad(11b)$$

In order to solve the over-determined equations, an objective function (F) is defined as the sum of the squared projections of the modified datum vectors on the shape-matrix vector,

$$\begin{aligned}F&=\sum_{i\in A}\left(v_i^{\mathrm{T}}b\right)^2+\sum_{i\in A_1\cup A_2}\left(w_i^{\mathrm{T}}b\right)^2\\&=\sum_{i\in A}b^{\mathrm{T}}v_iv_i^{\mathrm{T}}b+\sum_{i\in A_1\cup A_2}b^{\mathrm{T}}w_iw_i^{\mathrm{T}}b\\&=b^{\mathrm{T}}\left(\sum_{i\in A}v_iv_i^{\mathrm{T}}+\sum_{i\in A_1\cup A_2}w_iw_i^{\mathrm{T}}\right)b=b^{\mathrm{T}}Ub\end{aligned}\quad(12)$$

$$U=\sum_{i\in A}v_iv_i^{\mathrm{T}}+\sum_{i\in A_1\cup A_2}w_iw_i^{\mathrm{T}}\quad(13)$$

$$A=A_1\cup A_2\cup A_3\quad(14)$$

where A_1, A_2 and A_3 are referred to as the subsets of sectional measurements with three known variables such as θ_i, l_{i1}, and l_{i2}, with two known variables such as θ_i and R_i, and with a known variable θ_i, respectively.

By minimizing the objective function under the constraint of Eq. (9), we have an optimal solution of the shape-matrix vector. This changes the estimation of a strain ellipsoid into an optimization problem. For this kind of problem, as proved by Shan et al. (2003) and Fry (1999), the solution is the eigenvector associated with the least eigenvalue of the symmetrical matrix U. However, in relation to the optimal solution of the shape-matrix vector, the negative of it is also a solution. One of these leads to a realistic strain ellipsoid having all positive axial lengths, while the other leads to an unrealistic ellipsoid having at least one negative axial length. The latter is discarded.

4. Dimension determination of a strain ellipsoid

In the case of sectional measurements with three known variables such as θ_i, l_{i1}, and l_{i2}, Robin (2002) regarded l_{i1} and l_{i2} as two independent variables in calculating the absolute shape matrix. This may not be necessary because these two variables of a measured ellipse are closely related in dimension to those of other ellipses. This can be illustrated from Eq. (7d). In fact, an absolute strain ellipsoid can be estimated after obtaining a relative strain ellipsoid, as described below.

Through applying the proposed method to these data, an optimal solution of the shape-matrix vector, $b^* = [b^*_{11}, b^*_{12}, b^*_{13}, b^*_{22}, b^*_{23}, b^*_{33}]$, can be obtained. A relationship between the relative (b^*) and the absolute ($\overline{b}$) solutions is given as:

$$\overline{b} = k_i b^* \tag{15}$$

where k_i is the unknown scale parameter for the i-th measurement.

Inserting Eq. (15) into Eqs. (7a) and (7b) leads to the following expressions:

$$\left(t^{(i)}_{11}t^{(i)}_{11}b^*_{11} + 2t^{(i)}_{11}t^{(i)}_{21}b^*_{12} + 2t^{(i)}_{11}t^{(i)}_{31}b^*_{13} + t^{(i)}_{21}t^{(i)}_{21}b^*_{22} + 2t^{(i)}_{21}t^{(i)}_{31}b^*_{23} + t^{(i)}_{31}t^{(i)}_{31}b^*_{33}\right)k_i = l_{i2}^{-2} \tag{16a}$$

$$\left(t^{(i)}_{12}t^{(i)}_{12}b^*_{11} + 2t^{(i)}_{12}t^{(i)}_{22}b^*_{12} + 2t^{(i)}_{12}t^{(i)}_{32}b^*_{13} + t^{(i)}_{22}t^{(i)}_{22}b^*_{22} + 2t^{(i)}_{22}t^{(i)}_{32}b^*_{23} + t^{(i)}_{32}t^{(i)}_{32}b^*_{33}\right)k_i = l_{i1}^{-2} \tag{16b}$$

In terms of solving these two linear single-variable equations, there are many methods, such as the least square method, the moment method used above, and so forth. Among them, the least square method is adopted here, resulting in a simple estimate of the scale parameter k_i as follows:

$$k_i = \frac{p_i l_{i1}^{-2} + q_i l_{i2}^{-2}}{p_i^2 + q_i^2} \tag{17a}$$

$$p_i = t^{(i)}_{11}t^{(i)}_{11}b^*_{11} + 2t^{(i)}_{11}t^{(i)}_{21}b^*_{12} + 2t^{(i)}_{11}t^{(i)}_{31}b^*_{13} + t^{(i)}_{21}t^{(i)}_{21}b^*_{22} + 2t^{(i)}_{21}t^{(i)}_{31}b^*_{23} + t^{(i)}_{31}t^{(i)}_{31}b^*_{33} \tag{17b}$$

$$q_i = t^{(i)}_{12}t^{(i)}_{12}b^*_{11} + 2t^{(i)}_{12}t^{(i)}_{22}b^*_{12} + 2t^{(i)}_{12}t^{(i)}_{32}b^*_{13} + t^{(i)}_{22}t^{(i)}_{22}b^*_{22} + 2t^{(i)}_{22}t^{(i)}_{32}b^*_{23} + t^{(i)}_{32}t^{(i)}_{32}b^*_{33} \tag{17c}$$

5. Procedure for the proposed method

The procedure for the proposed method is described as follows.

(1) Eq. (3) is used to rotate each measured planar surface to the horizontal with the long axis directed toward the X-axis of the ellipse.
(2) Eq. (8a) and/or Eq. (8b) are used to calculate the coefficients of the linear equation(s) describing the rotated ellipse on the surface.
(3) The calculated coefficients are divided by their lengths so that the datum vector v_i and/or datum vector w_i are determined.
(4) Eq. (13) is used to calculate the elements of rank-6 matrix U.
(5) The Jacobian method is used to determine the eigenvalues and eigenvectors of the matrix.
(6) The least eigenvector is sought as an optimal solution of the shape-matrix vector b^*.
(7) Eq. (17) is used to estimate the scale parameter k_i.
(8) Eq. (1) is used to construct the shape matrix.
(9) From the constructed shape matrix, the directions and the magnitudes (see Eq. (2)) of the shape matrix are determined using the Jacobian method.

6. Examples

In order to demonstrate the feasibility of the proposed method, three artificial examples and one real example are used. The artificial examples (with and without measurement errors) were generated at random under a unique prescribed strain (Table 2).

6.1. Artificial examples without measurement errors

No measurement errors were included in the first and the second artificial examples. This is unrealistic but justifiable in validating the new method. For each controlled measurement, the planar surfaces were sampled evenly at random from 0° to 360° for dip directions and, from 0° to 90° for dip angles. The elements of strain ellipses were calculated under the prescribed strain tensor (Table 2).

The first artificial example consists of three strain measurements with two known variables such as θ_i and R_i (Table 3). Table 2 lists the results from applying this method. It is similar to the prescribed value, indicating that the method is feasible for determining a strain ellipsoid from sectional measurements. The close agreement between the prescribed and estimated strain ellipsoids results from the lack of measurement errors in this artificial data.

In the second artificial example, there are two kinds of measurements, with two known variables such as θ_i and R_i and with one known variable such as θ_i, having a data number of 2 and 3, respectively (Table 3). Strain inferred from these data through using the above method is listed in Table 2. This also does not differ from the prescribed strain.

6.2. Artificial example with measurement errors

The third artificial example has the same planar surfaces and the same axial ratios to those of the second example (Table 3). They only differ in the value of pitches. For the sake of simplicity, measurement errors are included by

Table 2
Prescribed and calculated strain ellipsoids

	Calculated strain ellipsoids										
	Maximum axis			Intermediate axis			Minimum axis			$\varepsilon_1/\varepsilon_2$	$\varepsilon_2/\varepsilon_3$
	Magnitude	Bearing (°)	Plunge (°)	Magnitude	Bearing (°)	Plunge (°)	Magnitude	Bearing (°)	Plunge (°)		
Prescribed	3.00	90.00	0.00	2.00	0.00	0.00	1.00	180.00	90.00	1.50	2.00
Our method											
Artificial											
1	3.06	90.00	0.00	2.04	0.00	0.00	1.02	180.00	90.00	1.50	2.00
2	3.06	90.00	0.00	2.04	0.00	0.00	1.02	180.00	90.00	1.50	2.00
3	3.01	267.39	1.09	1.99	177.39	0.28	1.02	73.26	88.72	1.52	1.95
Real	2.64	100.59	0.43	1.86	193.61	89.79	1.03	10.53	8.20	1.42	1.82
Zheng and Chang's (1985) result	1.38	279	3	1.27	155	84	0.66	9	4	1.1	1.9

The artificial and the real examples are listed in Table 3. ε_1, ε_2, and ε_3 are the corresponding half lengths of the maximum, the intermediate and the minimum strain axes. They are all relative in the examples. The real example is taken from Zheng and Chang (1985) whose result is shown in the last row. See the text for more explanation.

Table 3
Strain measurements in the artificial and the real examples

Examples	No	Planar surfaces		Strain ellipses	
		Dip direction α_i (°)	Dip angle β_i (°)	Pitch θ_i (°)	Axial ratio R_i
Artificial					
1	1	30.61	54.12	94.12	1.83
	2	348.46	17.07	22.61	1.18
	3	143.28	23.66	64.05	1.38
2	1	30.61	54.12	94.12	1.83
	2	348.46	17.07	22.61	1.18
	3	143.28	23.66	64.05	
	4	32.24	50.44	95.09	
	5	291.44	53.27	87.29	
3	1	30.62	54.12	96.12	1.83
	2	68.29	46.35	20.61	1.18
	3	267.66	8.06	62.05	
	4	291.44	53.27	97.09	
	5	358.23	65.36	85.29	
Real	1	305	78	82	1.92
	2	205	87	8	1.98
	3	133	9	54	1.95

Measurement errors do not exist in the first and the second artificial examples, but in the third artificial example. The real example is taken from Zheng and Chang (1985).

stochastically adding either 2° or −2° to the pitches of the second example. However, other ways or larger angular values may be considered to simulate measurement errors in data, but this is beyond the scope of this paper.

Application of the method to this example gives rise to the result listed in Table 2. The estimated strain ellipsoid closely resembles the prescribed one. The resemblance is due to the assignment of small measurement errors to the pitches.

6.3. Real example

The real example (Table 3) is taken from Zheng and Chang (1985). It consists of three sectional measurements of Carboniferous conglomerates in Zhoukoudian, west of Beijing. These sedimentary rocks, as a part of the cover of the North China platform, were slightly metamorphosed, and intensely deformed in the Triassic and Jurassic. Table 2 lists the results using the proposed method, and also that of Zheng and Chang (1985) who used the method of Gendzwill and Stauffer (1981). Both give similar principal directions (Fig. 2) and roughly similar axial ratios. The strain ellipsoid obtained by us and by Zheng and Chang (1985) has a Lode's parameter (Hossack, 1968) of −0.626 and −0.936, respectively. Both indicate a strain state of uniaxial apparent flattening.

Orife and Lisle (2003) suggested using stress difference to investigate the difference between two stress tensors (D). According to their statistical study, stress tensors are considered very similar if $D < 0.66$, similar if $0.66 < D < 1.01$, different if $1.01 < D < 1.71$, or very different if $D > 1.71$. This approach was used herein to quantify the similarity between

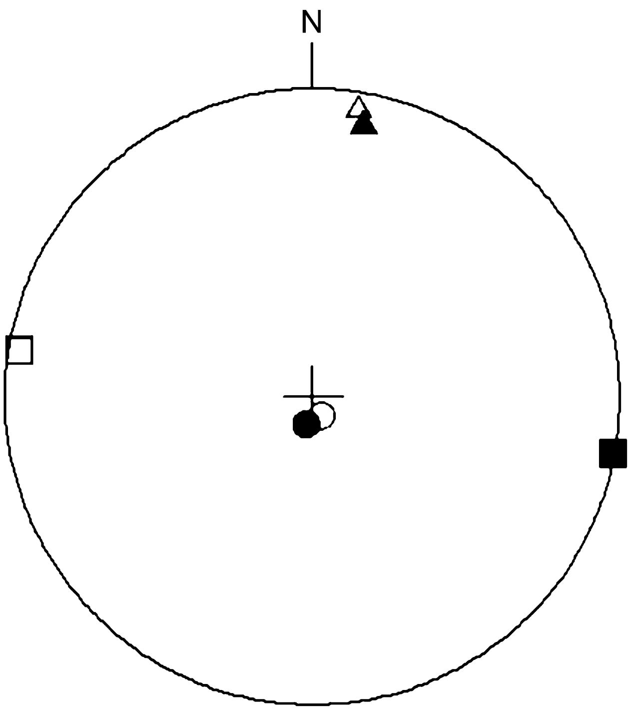

Fig. 2. Comparison between estimated principal directions (Table 2), using the proposed method (blank symbol) and the method of Gendzwill and Stauffer (1981) (black-filled symbol), respectively. Equal-area, lower-hemispheric projection. Rectangles, triangles, and circles represent the maximum, the intermediate and the minimum principal directions, respectively.

the two estimated strain ellipsoids. The calculated difference is 0.39, indicating the similarity between the two estimated strains.

However, the strain ellipsoid obtained in the above way differs slightly from that by Zheng and Chang (1985). The difference is mainly ascribed to measurement errors that lead to the inconsistency of strain ellipses in variable sections, and the use of differing algorithms in calculation.

7. Discussions and conclusions

A new method is developed in this paper to calculate a strain ellipsoid from strain measurements made on planar surfaces. For each measurement with known variable(s) such as θ_i or/and R_i, one or two linear equations describing the shape matrix are established. The linear character of these equations indicates that the shape-matrix vector is perpendicular to a hyperplane in a six-dimensional space consisting of six independent elements of the shape matrix. We have solved an optimal problem under the assumption that the shape-matrix vector can be located on a unit hyper-sphere centered at the origin. It is recognized that the eigenvector of data matrix associated with the least eigenvalue is an optimal solution of the shape-matrix vector. Application of this method to four examples has demonstrated its feasibility in determining a strain ellipsoid.

The proposed method and that of Robin (2002) are similar, in terms of directness and lack of iteration in calculation. However, the newer method is more flexible because more kinds of strain measurements can be considered. Three types of strain measurements are recognized: (A) measurements with three known variables such as θ_i, l_{i1}, and l_{i2} where the measured plane is through the center of the strain ellipsoid; (B) measurements with two known variables such as θ_i and R_i, and (C) measurements with a single known variable θ_i. Measurements of variable kinds are readily incorporated in the calculation of the strain ellipsoid by using the proposed method, whereas Robin's method can only deal with the first two types A and B. As shown herein, a relative strain ellipsoid and an absolute magnitude can be estimated separately. The former may be estimated analytically before obtaining the latter. It is not necessary during calculation to incorporate the scale parameter as an independent variable with the shape-matrix variables, as Robin (2002) did. This incorporation takes much more time and memory, although it is not a problem for modern high-speed, high capacity personal computers.

Table 4
Eigenvalues and eigenvectors of datum-vector matrix for two sets of measurements of the third kind

Data number	No	Eigenvalues	Eigenvectors					
			b_{11}	b_{12}	b_{13}	b_{22}	b_{23}	b_{33}
5	1	6.00981	0.32927	0.59499	−0.45097	−0.39024	−0.42213	0.06098
	2	2.25952	0.13048	0.59357	0.70372	−0.15464	0.33306	0.02416
	3	1.44555	−0.14799	0.31153	−0.54696	0.17540	0.74187	−0.02741
	4	0.28512	−0.51251	0.44341	0.04737	0.60742	−0.40063	−0.09491
	5	0.00000	0.76429	0.00000	0.00000	0.64487	0.00000	0.00004
	6	0.00000	−0.07650	0.00000	0.00000	0.09060	0.00000	0.99294
6	1	6.01085	0.32867	0.59476	−0.46062	−0.38953	−0.41308	0.06086
	2	3.45512	0.08742	0.06580	0.78073	−0.10361	−0.60621	0.01619
	3	2.16859	0.08600	0.64242	0.41276	−0.10192	0.63158	0.01593
	4	0.36543	−0.53568	0.47878	−0.08894	0.63488	−0.25098	−0.09920
	5	0.00000	0.76446	0.00000	0.00000	0.64467	0.00000	−0.00215
	6	0.00000	−0.07482	0.00000	0.00000	0.09202	0.00000	0.99294

The first set consists of five measurements extracted from the second artificial example (Table 3), while the second set is the first set and an additional measurement. The additional measurement, generated at the same prescribed strain, is 315.59° in dip direction, 89.96° in dip angle, and 89.96° in pitch. There is a shape-matrix vector of [0.10717, 0.00000, 0.00000, 0.24114, 0.00000, 0.96455] for the prescribed strain. Note the difference between it and one of the two eigenvectors related to the minimum eigenvalues.

For measurements made on plane surfaces that are not parallel to the principal planes, a minimum number of independent strain measurements are required to determine a strain ellipsoid. They are 2 and 3 for types A and B, respectively. The number depends on the type of strain measurement. The fewer elements of a strain ellipse measured on a planar surface, the more measurements are needed to determine the strain ellipsoid. Type A measurements are necessary to determine the absolute strain ellipsoid, while type B are needed to calculate the relative strain ellipsoid.

A problem arises over the independence of type C measurements in determining a strain ellipsoid. To show this issue, a set of type C measurements was extracted from the second artificial example (Table 3), and processed. In Table 4, both the two smallest eigenvalues of data matrix U are zero, indicating the existence of a two-dimensional subspace in which the objective function reaches minimum, or zero. Things never appear to change much if one or more measurement of this kind is added to the data set (Table 4). In such cases, the eigenvector related to the minimum eigenvalue is not always identical to the solution of the shape-matrix vector, analogous to the results from stress inversions (Shan and Fry, 2006). This underdeterminability is intrinsic in that Eq. (7) is satisfied by a strain state having the rock shrink or expand evenly in all directions. In this sense, type C measurements must be used together with either type A or B to determine the strain ellipsoid. The role played by type C measurements, when not in combination with other kinds, in reducing the parameter space, will be addressed elsewhere (Shan et al., submitted for publication).

Acknowledgements

This work is funded by the Hundred Talent Program of Chinese Academy of Sciences (KZCX0543081001), and the National Natural Science Foundation of China (Grant 40672144). Norman Fry and Chongbin Zhao helped check the written English of this paper. T.H. Bell, W.H. Owens, J. Hippertt, and one anonymous referee reviewed this paper, and made valuable suggestions and modifications to it.

References

De Paor, D.G., 1990. Determination of the triaxial strain ellipsoid from sectional data. Journal of Structural Geology 12, 131–137.

Gendzwill, D.J., Stauffer, M.R., 1981. Analysis of triaxial ellipsoids; their shapes, plane sections, and plane projections. Mathematical Geology 13, 135–152.

Fry, N., 1999. Striated faults: visual appreciation of their constraint on possible palaeostress tensors. Journal of Structural Geology 21, 7–22.

Hossack, J.R., 1968. Pebble deformation and thrusting in the Bygdin area (S. Norway). Tectonophysics 5, 315–339.

Milton, N.J., 1980. Determination of the strain ellipsoid from measurements on any three sections. Tectonophysics 64, T19–T27.

Oertel, G., 1978. Strain measurements from the measurement of pebble shapes. Tectonophysics 50, T1–T7.

Orife, T., Lisle, R.J., 2003. Numerical processing of palaeostress results. Journal of Structural Geology 25 (6), 949–957.

Owens, W.H., 1984. The calculation of a best-fit ellipsoid from elliptical sections on arbitrarily orientated planes. Journal of Structural Geology 6, 571–578.

Ramsay, J.G., 1967. Folding and Fracturing of Rocks. McGraw-Hill Book Company, New York, 568 pp.

Ramsay, J.G., Huber, M.I., 1983. The Techniques of Modern Structural Geology. In: Strain Analysis, vol. 1. Academic Press, London, 307 pp.

Robin, P.-Y.F., 2002. Determination of fabric and strain ellipsoids from measured sectional ellipses – theory. Journal of Structural Geology 24, 531–544.

Shan, Y., Fry, N., 2006. The moment method used to infer stress from fault/slip data in sigma space: invalidity and modification. Journal of Structural Geology 28, 1208–1213.

Shan, Y., Gong, F., Li, Z., Lin, G. Determination of strain principal directions from sectional measurements of stretch lineation. Journal of Structural Geology, Submitted for publication.

Shan, Y., Suen, H., Lin, G., 2003. Separation of polyphase fault/slip data: an objective-function algorithm based on hard division. Journal of Structural Geology 25, 829–840.

Shao, J., Wang, C., 1984. Determination of strain ellipsoid according to two-dimensional data on three or more intersection planes. Mathematical Geology 16, 823–833.

Shimamoto, T., Ikeda, Y., 1976. A simple algebraic method for strain estimation from ellipsoidal objects. Tectonophysics 36, 315–337.

Wheeler, J., 1989. A concise algebraic method for assessing strain in distributions of linear objects. Journal of Structural Geology 11, 1007–1010.

Zheng, Y., Chang, Z., 1985. Finite Strain Measurement and Ductile Shear Zones (in Chinese). Geological Publishing House, Beijing, 185 pp.